Optical Engineering

SPIEDigitalLibrary.org/oe

# Programmable diffractive lens for ophthalmic application

María S. Millán
Elisabet Pérez-Cabré
Lenny A. Romero
Natalia Ramírez

SPIE

# Programmable diffractive lens for ophthalmic application

**María S. Millán,* Elisabet Pérez-Cabré, Lenny A. Romero,† and Natalia Ramírez**
Universitat Politècnica de Catalunya, Department of Optics and Optometry, Applied Optics and Image Processing Group, 08222 Terrassa (Barcelona), Spain

**Abstract.** Pixelated liquid crystal displays have been widely used as spatial light modulators to implement programmable diffractive optical elements, particularly diffractive lenses. Many different applications of such components have been developed in information optics and optical processors that take advantage of their properties of great flexibility, easy and fast refreshment, and multiplexing capability in comparison with equivalent conventional refractive lenses. We explore the application of programmable diffractive lenses displayed on the pixelated screen of a liquid crystal on silicon spatial light modulator to ophthalmic optics. In particular, we consider the use of programmable diffractive lenses for the visual compensation of refractive errors (myopia, hypermetropia, astigmatism) and presbyopia. The principles of compensation are described and sketched using geometrical optics and paraxial ray tracing. For the proof of concept, a series of experiments with artificial eye in optical bench are conducted. We analyze the compensation precision in terms of optical power and compare the results with those obtained by means of conventional ophthalmic lenses. Practical considerations oriented to feasible applications are provided.  [DOI: 10.1117/1.OE.53.6.061709]

Keywords: ophthalmic lens; visual ametropia compensation; programmable lens; diffractive optical element; liquid crystal display; spatial light modulator.

Paper 131596SS received Oct. 21, 2013; revised manuscript received Dec. 22, 2013; accepted for publication Jan. 24, 2014; published online Mar. 18, 2014.

## 1 Introduction

Programmable diffractive lenses (also called phase Fresnel holograms/kinoform lenses, etc.)[1] displayed on pixelated liquid crystal devices are of common use in optical processors and information optics. Very often they are multiplexed to other elements such as filters or holograms so as to implement a complex diffractive optical element.[2–5] Despite their attractive properties of refreshment and flexible design, the application of programmable lenses to ophthalmic optics for compensation of visual ametropia is, however, very limited. Some liquid crystal devices have been already proposed for their use as spectacle lenses and some prototypes can be found in the literature.[6–9] They usually have a diffractive design, either displayed on a pixelated device,[5,8] or on a device consisting of other arrays of cells (e.g., with circular symmetry in Ref. 9). A commercially available eyewear system targets presbyopia by means of a progressive-addition lens that contains a liquid crystal device layer. The lens is controlled electronically and changes from full distance viewing prescription to near focus prescription depending on the head movement.[10] Very intense research activity has been developed in the field and, among the published contributions, it is worth mentioning an apparatus based on a liquid crystal programmable phase modulator proposed as an adaptive optics tool in the early stages of the design of ophthalmic optical elements with increased depth of field for presbyopic subjects.[11] The system has been further developed for wave-aberration control[12] and binocular adaptive optics vision analysis.[13]

Some practical difficulties arise when considering the ophthalmic application of programmable lenses displayed on liquid crystal devices: low efficiency, chromatic aberrations (more important with diffractive designs), polarized light requirements, etc. The valuable properties of a programmable diffractive lens can be achieved when it is displayed on a pixelated liquid crystal screen that acts as a phase only light modulator. Modern liquid crystal on silicon (LCoS) devices exceed $2\pi$-phase modulation with almost inexistent amplitude coupled modulation, high efficiency, and small pixel pitch (of 8 $\mu$m or even smaller[14]) so that it is possible to generate lenses of higher powers (for instance, powers up to 9 D for a wavelength of 633 nm are justified in Sec. 2). On the other hand, these electronic addressed devices are typically reflective, have relatively small aperture (1 cm $\times$ 2 cm, approximately), and require an associated control system. In practice, the mechanical and electronic requirements of these spatial light modulators (SLMs) in their current state-of-the-art would cause many limitations to the user in their mobility. For example, a reflective system requires additional optics to place the SLM conjugate pupil making mobile devices impractical. All these constraints explain that programmable lenses have been considered of little usefulness for ophthalmic applications. But, apart from spectacles and adaptive optics vision analyzers, there are other ophthalmic applications that may still be matter of interest. For instance, programmable lenses can be inserted in the eyepieces of optical instruments or in phoropters for optometric assessment of visual acuity. In these cases, the use of diffractive programmable lenses would potentially compensate for the possible visual refractive error of the observer (or patient) with more precision than current devices. Although high quality eyepieces show a range of some $\pm$diopters (D) for compensating relatively low myopia or hypermetropia, they cannot compensate for astigmatism or presbyopia or

*Address all correspondence to: María S. Millán: millan@oo.upc.edu

†Current address: Universidad Tecnológica de Bolívar, Ciencias Básicas, Cartagena de Indias, Colombia

0091-3286/2014/$25.00 © 2014 SPIE

high-order aberrations. Optometrists usually introduce one or more trial-set lenses of relative small aperture in phoropters or trial frames for the assessment of visual acuity. These trial-set lenses are graded in steps of 0.25 D thus establishing a limit for the uncertainty of the assessment.[15]

In this work, we explore the potential capability of programmable diffractive lenses displayed on a pixelated and reflective LCoS device to quickly determine and compensate for the refractive error of the observer eye. The programmable lens displayed on an LCoS light modulator is a non-moving component proposed as an alternative element to the common ophthalmic lens—or group of ophthalmic lenses—currently used for visual compensation in, for instance, a phoropter for optometric visual assessment. We consider common ametropies (such as myopia, hypermetropia, and astigmatism) and presbyopia. For the experimental proof of concept, we use an artificial eye in optical bench. The artificial eye is initially adjusted as to be emmetropic. Placing an additional lens with the appropriate adding power before it, the artificial eye can simulate an eye affected by either myopia, or hypermetropia, or astigmatism, or presbyopia. The LCoS-SLM is then programmed to display a series of lenses to compensate for the disorder introduced in the artificial eye. A fine-tuning of the optical power (focal length) of the programmable diffractive lens allows the compensation of the ametropic eye without the need of replacing or moving any element or physically trying with lenses of different powers. We compare the compensation achieved by the programmable lens displayed on the LCoS device with the compensation achieved by introducing a conventional ophthalmic lens from a trial lens case. To this end, we use the USAF resolution test chart (set by the United States Air Force in 1951) as the object for imaging. The modulation transfer function (MTF) is also computed and used for the comparison of both kinds of compensation.

## 2 Theoretical Background

### 2.1 *Programmable Phase Fresnel Lens*

Let us denote the quadratic phase pattern of a spherical lens, in spatial coordinate ($x_0$) and with focal length $f$, by $l(x_0, f)$, which is the continuous function

$$l(x_0, f) = \exp\left(-\frac{j\pi}{\lambda f}x_0^2\right) \tag{1}$$

represented in one spatial dimension for the sake of simplicity. The wavelength of the design is represented by $\lambda$. The pixelated structure of the SLM is responsible for a spatial discretization of the phase distribution displayed on the modulator. This discrete distribution can be written as

$$l(m, f) = \exp\left(-\frac{j\pi}{\lambda f}\frac{L^2}{N_1^2}m^2\right) \quad \forall\, m \in \left[-\frac{N_1}{2}+1, \frac{N_1}{2}\right], \tag{2}$$

where $m$ is the pixel position and $L$ is the diameter of the lens aperture that corresponds to a given number of pixels $N_1$. In general, $L \le L_0$, where $L_0$ is the total SLM aperture. As Eq. (2) reveals, the phase value varies more rapidly in the periphery than in the center of the lens aperture (Fig. 1). According to the Nyquist criterion, the phase shift between two neighbor pixels of Eq. (2) at the border of the lens aperture must be lower than or equal to $\pi$.[16,17] This condition results in a minimum value for the focal length, named the reference focal length, of the programmable lens. For a given SLM, with a particular pixel pitch, the requirement establishes that the sampling frequency fits for the Nyquist criterion at the borders of the lens aperture. Assuming that $L = N_1\delta x_0$, where $\delta x_0$ is the pixel pitch, the reference focal length $f_{\text{ref}}$, or equivalently, the reference power, can be determined from the expression[16,17]

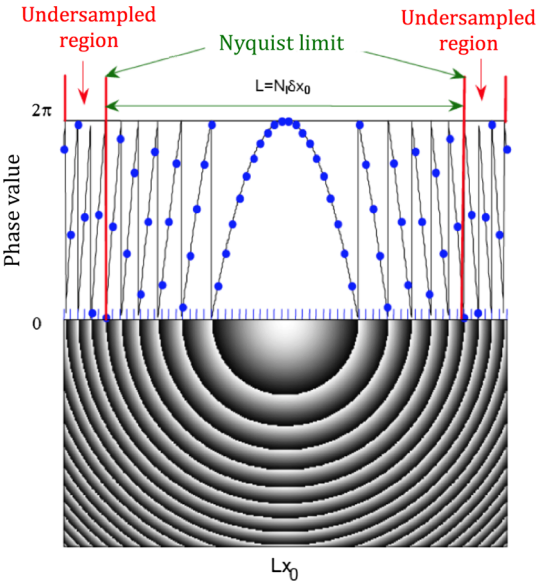


**Fig. 1** Spatial discretization and phase profile of a (modulo-$2\pi$) programmable lens addressed to an SLM. Blue dots represent the phase values addressed to the elements of the pixelated screen after the spatial discretization and phase quantization of the continuous phase profile (in solid black line). Vertical red lines indicate the maximum lens aperture that fits the Nyquist criterion.

$$f_{\text{ref}} = \frac{N_1}{\lambda}\delta x_0^2. \tag{3}$$

For instance, taking into account the specifications of the Holoeye LCoS-SLM used in this work ($N_1 = 1080$, $\delta x_0 = 8\ \mu$m) and $\lambda = 633$ nm, we obtain an $f_{\text{ref}} = 0.109$ m or, equivalently, an optical power of 9.16 D. We assume that the SLM works in phase-only regime, with a minimal amplitude modulation and a linear phase response. We also assume that the phase modulation range is restricted to $2\pi$ radians (modulo-$2\pi$), which corresponds to the phase modulation depth available to reproduce the programmed phase lens with, for instance, a focal length of $f = f_{\text{ref}}$. Furthermore, the phase modulation range is usually discretized into a number of levels addressable through the video graphic array card. In our experiments, 256 discrete phase levels were available.

### 2.2 *Compensation of Refractive Errors Induced in an Artificial Eye*

Let us recall the principles for the compensation of refractive errors known as ametropia in human eyes. Many model eyes have been reported (see, for instance, Refs. 18 and 19); however, for the proof of concept described in this work, we consider an over-simplified version of the eye, hereafter named artificial eye [Fig. 2(a)], consisting of a photographic objective lens with 55 mm effective focal length and $f/2.8$ ($L_{\text{ob}}$ in

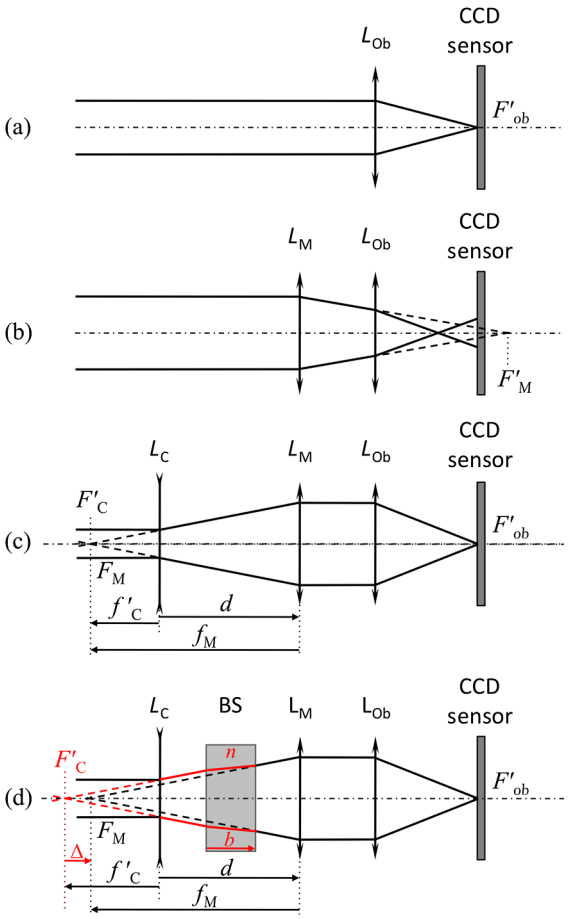


**Fig. 2** Simulation of an artificial myopic eye on an optical bench and its ophthalmic compensation. (a) Emmetropic eye; (b) myopic eye (myopia induced by lens $L_M$); (c) myopia compensation by lens $L_C$; (d) longitudinal displacement, $\Delta$, introduced by the plano-parallel plate effect of the beam splitter (BS).

Fig. 2) and a CCD sensor. The photographic objective lens simulates the optical system of the eye whereas the CCD sensor plays the role of the retina. The artificial eye is first adjusted so as to be emmetropic. It means that the relative position of the lens $L_{ob}$ and the CCD sensor is fixed so that a distant object (i.e., at infinity) is focused on the CCD sensor placed at the second focal plane of the objective, $F'_{ob}$, in the same way that an emmetropic eye sharply focuses the image of such a distant object on the retina. Different refractive errors (myopia, hypermetropia, and astigmatism) along with presbyopia can be simulated using this artificial eye in an optical bench.

### 2.2.1 *Myopia*

A myopic eye has higher optical power than an emmetropic eye. For a myopic eye, the image of a distant object will be focused in front of the retina, so that the CCD sensor captures a blurred image. As depicted in Fig. 2(b), the introduction of an additional converging lens, $L_M$, permits us to induce myopia to the emmetropic artificial eye in the optical bench. As a consequence, the artificial eye becomes myopic.

In order to compensate the artificial myopic eye for the induced refractive error, a third lens can be placed in front of the simulated eye. A compensating diverging lens, $L_C$, with appropriate power, can compensate for the myopia induced by $L_M$, provided that the second focal point of $L_C$ coincides with the first focal point of $L_M$, i.e., the condition $F'_C = F_M$ is fulfilled [see Fig. 2(c)]. Taking into account the distance $d$ between $L_C$ and $L_M$ and the refractive power of $L_M$, it is possible to compute the refractive power of $L_C$, or equivalently its focal length $f'_C$, to restore a sharp, focused final image at the CCD sensor plane. Thus

$$f'_C = f_X + d, \tag{4}$$

being $f_X$ the first focal length of the lens that induces the ametropia, $L_X$ (with $f'_X = -f_X$). In this case, $L_X = L_M$ and $f_X = f_M$ for induced myopia and the coordinate origin of each distance is indicated in Fig. 2(c). Distances measured in the same direction of the incident light are positive; otherwise, are negative.

### 2.2.2 *Hypermetropia*

Since a hypermetropic eye has lower optical power than an emmetropic eye, the image of a distant object through a hypermetropic eye is focused behind the retina. In analogous representation to Fig. 2, Fig. 3(b) shows how hypermetropia can be induced in the artificial emmetropic eye [Fig. 3(a)] by the use of a diverging lens, $L_H$. Analogously to the case of myopia, a compensating lens $L_C$, with appropriate power,

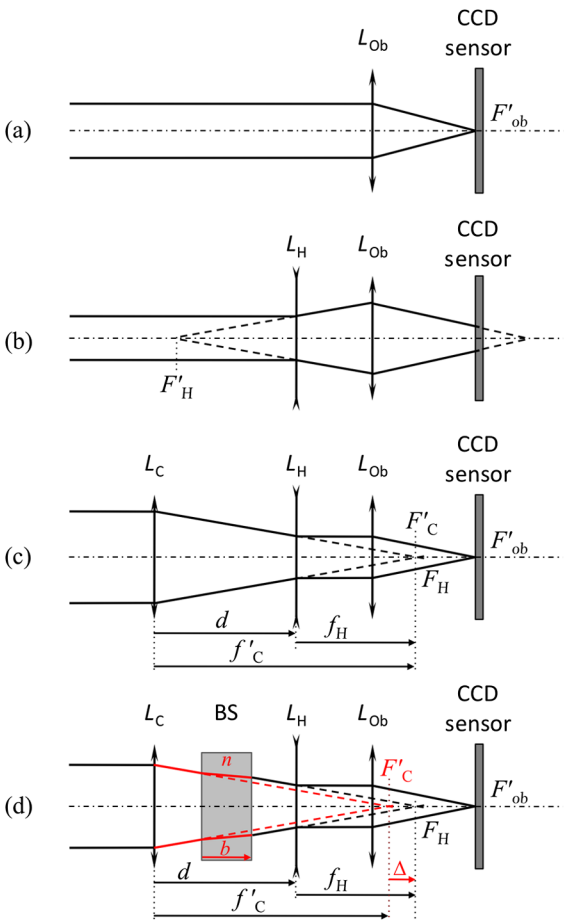


**Fig. 3** Simulation of an artificial hypermetropic eye on an optical bench and its ophthalmic compensation. (a) Emmetropic eye; (b) hypermetropic eye (hypermetropia induced by lens $L_H$); (c) hypermetropia compensation by lens $L_C$; and (d) longitudinal displacement, $\Delta$, introduced by the plano-parallel plate effect of the BS.

can compensate for the hypermetropia induced by $L_H$, provided that the second focal point of $L_C$ coincides with the first focal point of $L_H$, i.e., the condition $F'_C = F_H$ is fulfilled [see Fig. 3(c)]. The lens $L_C$ that compensates for hypermetropia must be converging. If the condition is met, a sharp image will be obtained in the CCD sensor plane. In terms of distances, the condition to obtain a sharp, focused image in the sensor plane of the compensated hypermetropic artificial eye is expressed by Eq. (4) with $f_X = f_H$.

### 2.2.3 *Astigmatism*

The introduction of a cylindrical lens $L_A$ in front of the artificial emmetropic eye permits to induce astigmatism. With the use of sphero-cylindrical or plano-cylindrical lenses in the position of $L_X$, a variety of cases can be simulated and described in terms of $L_M$ (Fig. 2) and $L_H$ (Fig. 3) for the principal meridians: from compound myopic astigmatism up to compound hypermetropic astigmatism, passing through simple myopic astigmatism, mixed astigmatism, and simple hypermetropic astigmatism. Applying in-plane rotations to the astigmatic lens $L_A$, we change the axis direction, or equivalently, the weaker and stronger principal meridians of the artificial astigmatic eye.[20] As a consequence of the induced astigmatism, the CCD sensor captures blurred images. Although they appear to be different from the defocused images caused by simple spherical ametropia (i.e., myopia or hypermetropia), the compensation of the induced astigmatism does not involve, from the conceptual point of view, a rather different solution. The compensation with the lens $L_C$ can be achieved by taking into separate consideration the two principal meridians of the artificial astigmatic eye. The compensating lens is, in turn, astigmatic, and its power in each principal meridian must meet the condition represented by Eq. (4). Apart from the blurring effects in the uncorrected astigmatic eye, there is some distortion in the image because of the different magnifications in the two principal meridians. After correction, a sharp image is restored, but, depending on the severity of astigmatism (i.e., the difference of power between the principal meridians) and the power and position of $L_C$, some residual distortion may still affect the final image.

### 2.2.4 *Presbyopia*

The young eye is able to increase its power (accommodation) by modifying the curvature of the crystalline lens, and consequently, it is able of focusing on objects placed at different distances. Presbyopia (from Greek roots meaning old eye) is a decline in this focusing ability that appears as the crystalline lens ages. Therefore, when the emmetropic eye becomes additionally presbyopic, it needs an extra focusing power in the form of a "near addition" of positive power. If the presbyopic eye is either myopic or hypermetropic, it needs two kinds of compensations: to focus distant objects (distance correction) and to focus close objects (near addition). The near addition of positive power is added to the distance correction.[20] The need for a near addition depends on both the available amplitude of accommodation and the application demands (i.e., the working distance for the near visual task).

It is possible to simulate this situation in an optical bench by placing the object test at a relatively close distance from the artificial eye (Fig. 4), for instance, about 10 times its focal length. A "young" emmetropic artificial eye would

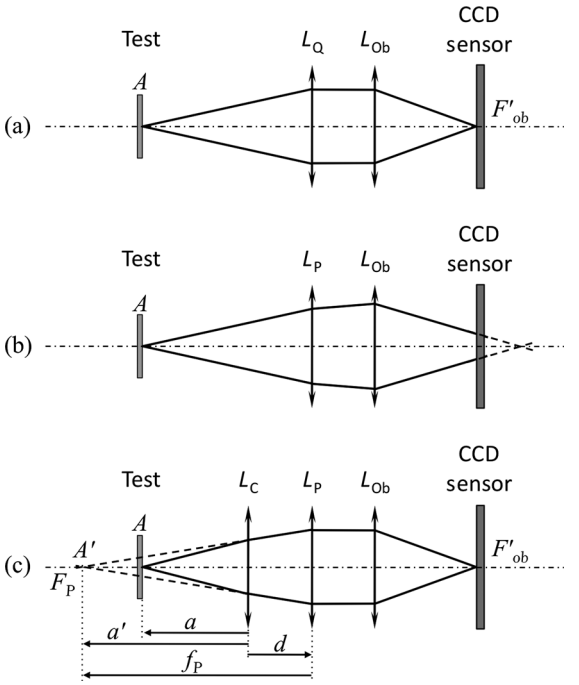


**Fig. 4** Simulation of presbyopia on an optical bench and its ophthalmic compensation. (a) Accommodated eye with the object test placed at near distance. $L_Q$ provides the necessary additional optical power to the emmetropic eye represented by $L_{ob}$ and the CCD sensor. (b) Presbyopic eye. The additional optical power of $L_P$ is under demand and the final image cannot be properly focused on the sensor. (c) Presbyopic eye compensated with the additional optical power of lens $L_C$ that brings again the focused image to the sensor plane.

accommodate, that is, would increase its power [represented by the converging lens $L_Q$ in Fig. 4(a)] to focus correctly the object on the sensor. However, an "old" emmetropic eye that suffers from presbyopia has insufficient amplitude of accommodation, and the power increase [represented by the lens $L_P$ in Fig. 4(b)] is below demand. In such a situation, the presbyopic artificial eye forms the image behind the CCD sensor, thus capturing a blurred image of the object. This loss in the available amplitude of accommodation can be compensated by an additional converging lens, $L_C$, placed in front of the presbyopic artificial eye. This lens images the near object test, located at a distance $a$, onto the first focal plane of lens $L_P$, thus obtaining a sharp final image in the sensor plane [Fig. 4(c)]. The refractive power of the compensating lens $L_C$ must be adjusted so that the lens equation

$$-\frac{1}{a}+\frac{1}{a'}=\frac{1}{f'_C} \tag{5}$$

is fulfilled, and the condition for the image distance $a' = f_P + d$ is satisfied [Fig. 4(c)].

## 3 Optical Experiment and Results

In this section, we first describe the optical setup used for the experiment. Second, we show the experimental results of the simulated spherical ametropies, astigmatism, and presbyopia and their compensation for an artificial eye. Two kinds of compensating lenses are used and compared: a programmable lens displayed on the LCoS-SLM and controlled by

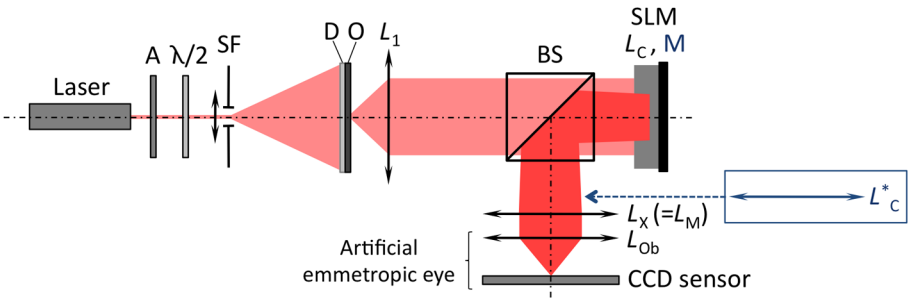


**Fig. 5** Optical setup used in the experiment: A-attenuator, $\lambda/2$-retarder half-wave plate, SF-microscope objective combined with a spatial filter, D-rotating diffuser, O-object test, $L_1$-collimating lens, BS-beam splitter, SLM-spatial light modulator acting either as a programmable compensating lens ($L_C$) or a flat mirror (M), $L_X$-lens inducing the refractive error (being X = M, H, A, or P for a myopic, hypermetropic, astigmatic, or presbyopic eye, respectively), $L_{ob}$-photographic objective and CCD sensor. When the trial lens was to be used for compensating the refractive error, $L^*_C$ was inserted closely before $L_X$ and, at the same time, the SLM was programmed to act as a flat mirror (M).

computer, and a set of conventional ophthalmic lenses from a trial lens case.

### 3.1 *Optical Setup*

Figure 5 shows the setup used in the experiment. A polarized He-Ne laser beam is used for the light source. An attenuator (A) allows a smooth control of the light intensity that reaches the CCD sensor. A retarder half-wave plate ($\lambda/2$) permits to carefully choose the polarization plane so that the LCoS-SLM achieves its best performance in phase-only modulation regime, which is above $2\pi$. An inverted microscope objective and a spatial filter allow us to expand the laser beam, which illuminates a rotating diffuser (D) next to the object test (O). This object is then illuminated with spatially incoherent light. The object is placed at the first focal plane of the collimating lens $L_1$. This lens forms the image of the test at infinity, which in turn, becomes the distant object test for the artificial eye. The standard USAF test imaged on the CCD sensor of the artificial emmetropic eye is shown in Fig. 6(a). The quality of this experimental image is evaluated through its MTF curve [Fig. 6(b)], which has been computed from a slanted edge of the USAF square element. To simulate a near object test, we move the lens $L_1$ toward the object test, so that the image is then formed at a closer distance from the artificial eye. The latter situation is to be used in the simulation of a presbyopic artificial eye.

The SLM used to display the programmable compensating lens in our experiments, $L_C$, is an LCoS device that works in reflective mode. For this reason, a nonpolarizing beam splitter (BS) cube is introduced in the setup to permit the incident beam to reach the SLM without modification of its polarization plane. After reflection in the SLM, the BS reflects part of the modulated beam toward the artificial eye. The emmetropic artificial eye is represented in Fig. 5 by the combination of a lens (a photographic objective, $L_{ob}$) and a CCD sensor. Throughout the experiments, this

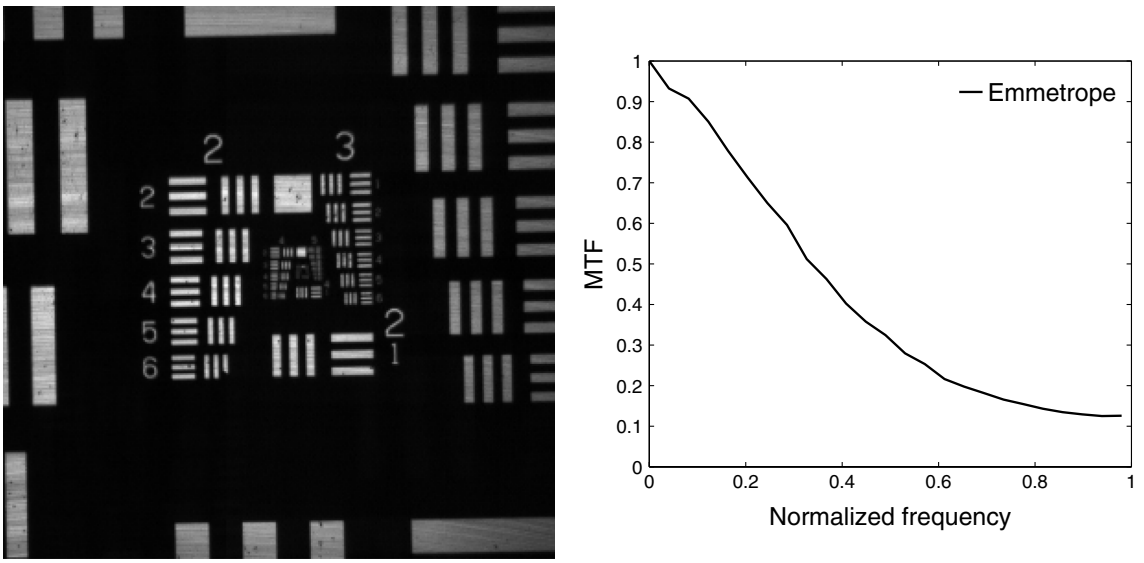


(a) (b)

**Fig. 6** (a) Experimental image of the standard 1951 USAF test chart captured by the CCD sensor of the artificial emmetropic eye. Only the central area of the image is displayed. White zones do not appear entirely uniform as an effect caused by the rotating diffuser placed against the test. (b) MTF curve of (a) that gives a reference of the initial image quality.

artificial eye is going to be affected by myopia, hypermetropia, astigmatism, or presbyopia. The lens that modifies the emmetropic eye to induce some of these dysfunctions is represented by $L_X$ (being X = M, H, A, and P to indicate myopia, hypermetropia, astigmatism, and presbyopia, respectively) in Fig. 5.

The SLM used in the experiment is a Holoeye high-definition television phase-only LCoS panel, model HEO 1080P, which has an active area of $15.36 \times 8.64$ mm$^2$, with a resolution of $1920 \times 1080$ pixels and 8.0 $\mu$m pixel pitch. A previous calibration of the device allowed us to establish the phase modulation linear range achievable by this SLM and the complete compensation for the LCoS panel surface deformation inherent to its fabrication process. A maximum phase modulation depth of $2.8\pi$ is achieved with an 8-bit electrical addressing (256 phase levels) via digital video interface for the impinging wavelength of $\lambda = 632.8$ nm (He-Ne laser).[21]

Eye dysfunction correction can be achieved by using a programmable compensating lens with the appropriate power displayed on the SLM ($L_C$ in Fig. 5) or, alternatively, by a conventional ophthalmic trial lens ($L_C^*$ in Fig. 5). In the latter case, the compensating lens $L_C^*$ would be inserted at a short distance in front of $L_X$—like a spectacle glass—at the same time that a constant phase value needs to be addressed to the SLM that would then act as a flat mirror ($M$ in Fig. 5). Let us make two comments derived from practical considerations on the experimental setup. For the first comment, the compensating lenses $L_C$ and $L_C^*$ would not have exactly the same power because of the different distances they are from the artificial eye. For the second comment, the presence of a BS in the ray path, between the SLM and the artificial eye, introduces a longitudinal displacement in the position of the second focal point of the compensating programmable lens $L_C$. The plane parallel plate equivalent to the right angle reflection prism of the BS produces such a displacement, which has to be taken into account in the refined calculation of the compensating power. Figures 2(d) and 3(d) show schematics of the influence of this displacement in the correction of myopia and hypermetropia, respectively. The longitudinal shift $\Delta$ can be computed by the expression

$$\Delta = \frac{n-1}{n} b, \tag{6}$$

where $n$ and $b$ denote the refraction index and the BS cube size, respectively. Taking into account that the BS in the setup has a $b = 50$ mm size and is made of BK7 material with $n = 1.52$, the resulting displacement is $\Delta = 17.1$ mm.

For both cases, myopia and hypermetropia [Figs. 2(d) and 3(d)], this shift will modify the focal length of the programmed lens $f'_C$ by

$$f'_C = f_X + d - \Delta, \tag{7}$$

where $f_X$ will be $f_M$ or $f_H$ in case of myopia or hypermetropia, respectively. Equation (7) is valid for compensating the astigmatism as well because it can be described in terms of $L_M$ and $L_H$ in the principal meridians separately.

### 3.2 *Experimental Results*

The setup shown in Fig. 5 has been used as proof of concept of the programmable lens displayed on the LCoS phase-only panel acting as a compensating lens for refractive errors and presbyopia.

In our series of experiments, myopia is the first ametropia induced in the artificial eye of the setup. A +3 D optical power lens $L_X = L_M$ is located in front of the emmetropic eye according to the schematic diagram of Fig. 5. The defocused image captured at the CCD sensor plane is shown in Fig. 7(a, left). The first focal length of $L_M$ is $f_M = -f'_M = -333.3$ mm. Distance $d$ from $L_M$ to $L_C$, which is the lens displayed in the SLM, is approximately $d = 90$ mm.

Let us first compensate for the refractive error by a programmable lens $L_C$ displayed on the SLM. According to Eq. (7), the second focal length of the diffractive lens should be $f'_C = -260$ mm. The distance values used to estimate $f'_C$ were approximated, not highly precise measurements, and therefore, some relatively small differences from the theoretical value could be expected. For this reason, small variations on the second focal length of $L_C$ were tried from the calculated value, and the best compensation, from visual inspection of the video images captured by the CCD, was experimentally obtained for $f'_C = -276$ mm, which is in fairly good agreement with the predicted theoretical value. The obtained image is shown in Fig. 7(b, left). We can see a significant improvement of the captured image when the programmable lens displayed on the SLM is finely tuned to compensate for the induced ametropia.

Alternatively, let us compensate for the refractive error with a conventional trial lens $L_C^*$ placed in front of the myopic eye while the SLM acts as a flat mirror (M in Fig. 5). Let us consider that the trial lens is placed at a distance $d = 10$ mm approximately. According to Eq. (4), a focal length of $-323$ mm should be used, which is equivalent to an optical power of $-3.09$ D. However, the set of trial lenses varies in quarter-diopter steps, thus, being an optical power of $-3$ D the closest value for the available lens of the trial set. Therefore, the ophthalmic lens of $-3$ D optical power (focal length of $-333.3$ mm) was located at the position of $L_C^*$ of Fig. 5. The experimental image captured by the compensated artificial eye is displayed in Fig. 7(c, left). It probes that myopia compensation was also achieved with the ophthalmic trial lens although with slightly lower quality in the resulting image.

In order to quantitatively compare the results obtained with both compensations, the MTFs were computed from a slanted edge of the USAF square element and the obtained curves were plotted in Fig. 7(d) along with the MTF curve for the emmetropic eye [Fig. 6(b)]. Despite experimental fluctuations, the MTF values for the compensation with the programmable lens (solid blue line) are very similar to the MTF of the emmetropic eye (dotted line), and above the equivalent MTF values for ophthalmic compensation (solid red line), thus indicating its slightly better performance as a compensating lens in comparison to the conventional ophthalmic trial lens. Although the available trial lenses are graded in steps of a quarter-diopter, a finer compensation could be obtained by slightly displacing $L_C^*$ from its position, in front of the artificial eye, and by shifting it along the optical axis. However, this option was discarded because it is not commonly considered when such trial lenses are inserted in phoropters or trial spectacle frames in the clinical practice.

The same experiment was repeated for a hypermetropic eye. A $-3$ D power lens ($L_H$) was then introduced in the

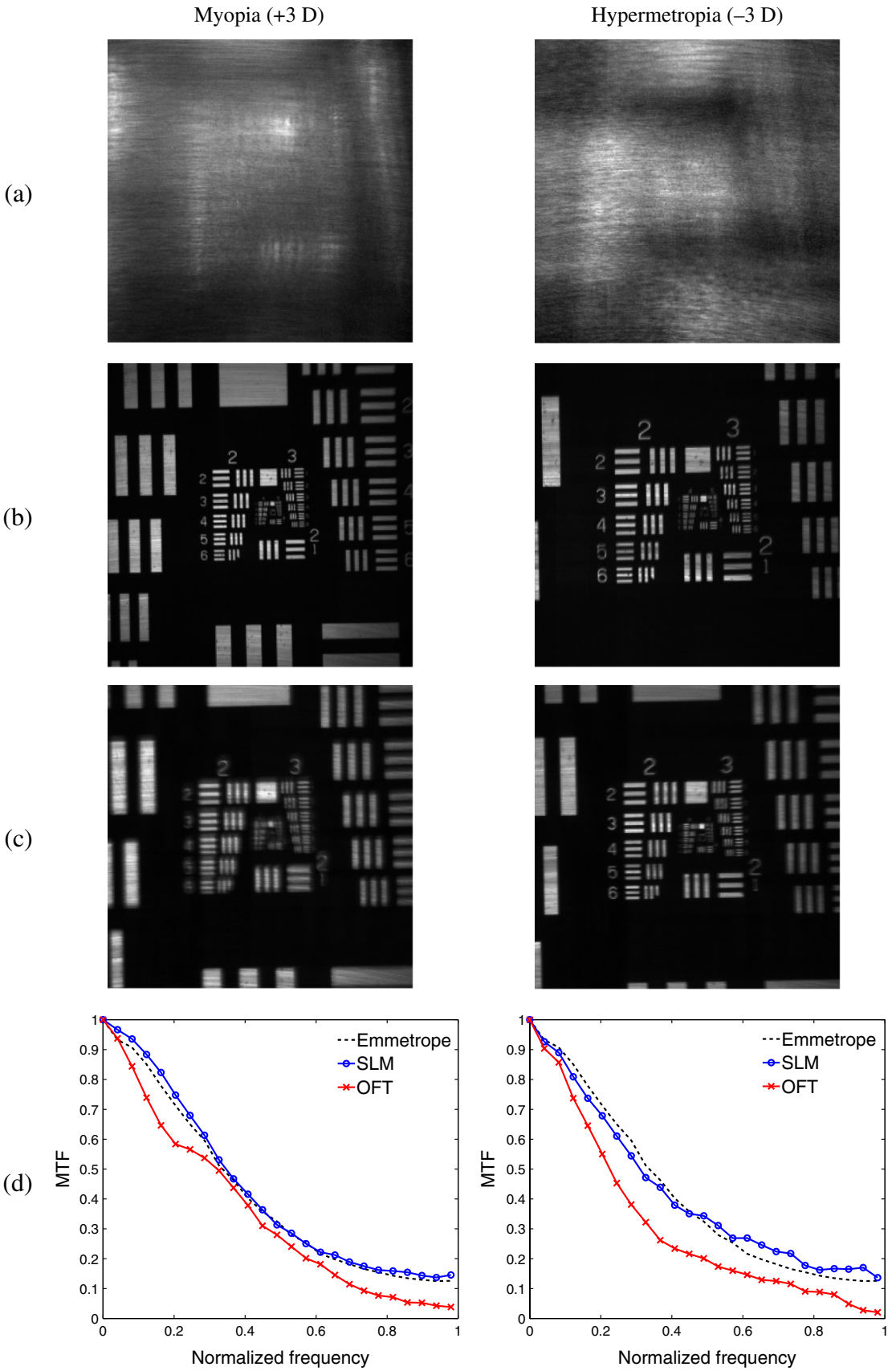


**Fig. 7** Experimental results for the compensation of the myopic eye (left) and the hypermetropic eye (right). (a) Defocused image due to the induced refractive error; (b) focused image obtained on the CCD sensor when the compensation was done by displaying a programmable lens on the SLM; (c) idem by using a conventional ophthalmic trial lens; (d) MTF functions computed from the focused images (b) and (c) along with the MTF of the emmetropic eye [Fig. 6(b)].

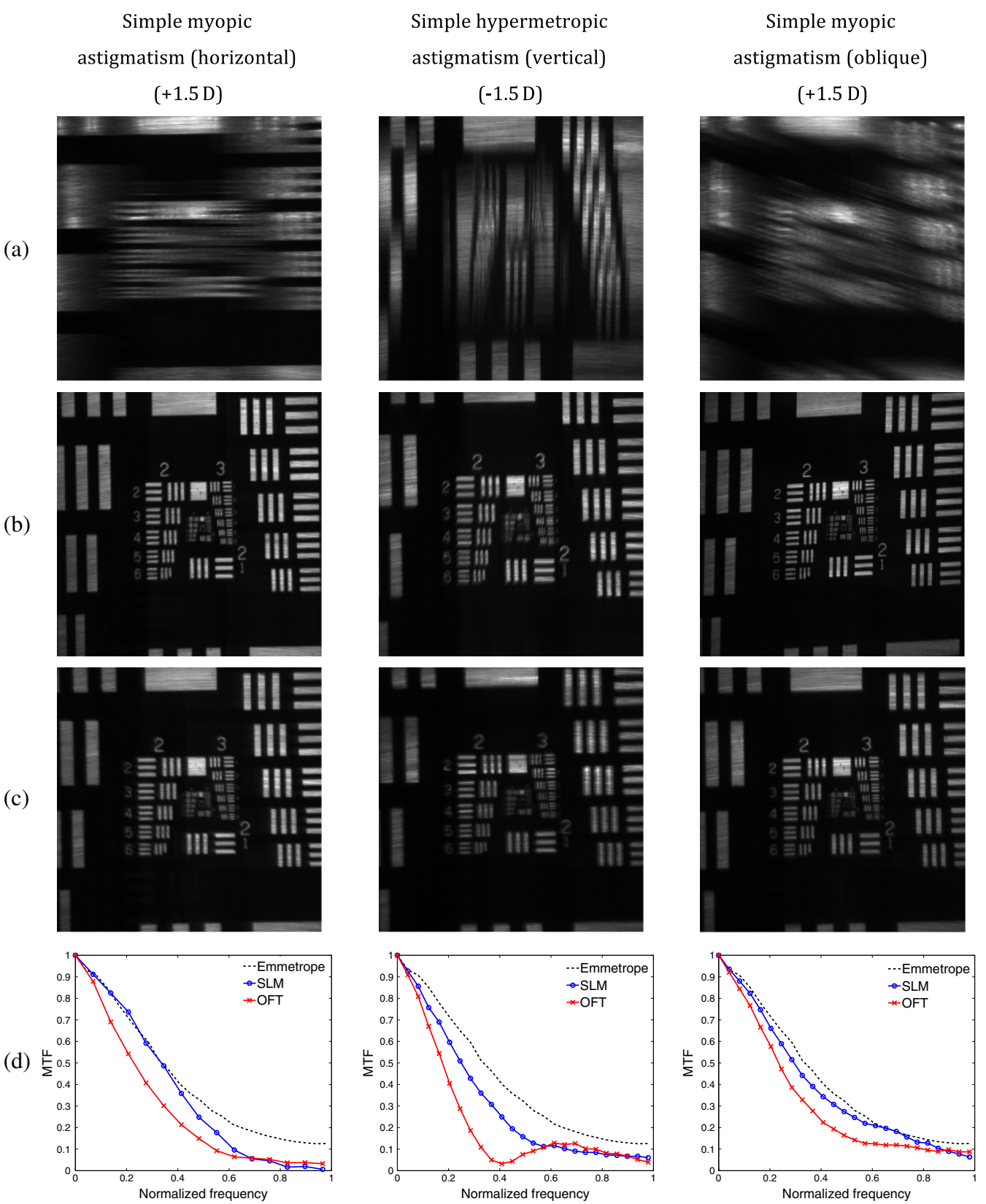


**Fig. 8** Experimental results for the compensation of the induced simple myopic astigmatism in the horizontal direction (left), simple hypermetropic astigmatism in the vertical direction (center), and simple myopic astigmatism in an oblique direction (right). (a) Defocused image due to the induced astigmatism; Focused image obtained in the CCD sensor when the compensation was done by (b) displaying a programmable lens on the SLM or, (c) using an ophthalmic cylindrical lens; (d) MTF functions computed from the focused images (b) and (c), along with the MTF of the emmetropic eye [Fig. 6(b)].

setup, at the position of $L_X$ indicated in Fig. 5, to induce hypermetropia to the artificial emmetropic eye. The defocused image obtained in this case is shown in Fig. 7(a, right). The first focal length of $L_H$ is $f_H = -f'_H = 333.3$ mm and distance from $L_H$ to $L_C$ is fixed to $d = 90$ mm. Thus, according to Eq. (7), the calculated focal length for the compensating programmable lens displayed on the SLM should be $f'_C = 406$ mm. The best-focused image was experimentally obtained for $f'_C = 400$ mm, which nearly coincides with the predicted focal length. Figure 7(b, right) displays this image as captured by the CCD sensor, where a clear improvement can be noticed with sharp contours and well-defined details.

The compensation of the hypermetropia was alternatively carried out using an ophthalmic trial lens. The trial lens was placed at $d = 10$ mm while a flat mirror was displayed on the SLM. According to Eq. (4), a focal length of +343 mm was necessary to compensate for the induced hypermetropia, which is equivalent to an optical power of +2.91 D. However, the closest ophthalmic lens available in the trial set had an optical power of +3 D. Ametropia compensation was also achieved as it can be seen from Fig. 7(c, right). The quality of this image is compared to the image obtained with the compensating programmable lens, by means of the MTF analysis. The corresponding MTF curves are plotted in Fig. 7(d), which show that the programmable lens performed better than the ophthalmic trial lens. From the same figure, it can be remarked that the programmable lens performed closely to the artificial emmetropic eye.

The third experiment deals with the compensation for induced astigmatism. Cylindrical ophthalmic lenses were successively placed in front of the emmetropic eye to simulate simple astigmatism in different directions ($L_X = L_A$ in Fig. 5). Simple myopic astigmatism in the horizontal direction was induced by inserting a +1.5 D cylindrical lens (first focal length $f_A = -666.6$ mm), whereas simple hypermetropic astigmatism in the vertical direction was induced by inserting a −1.5 D cylindrical lens (first focal length $f_A = +666.6$ mm). Left and central columns of Fig. 8(a) show the corresponding defocused images as they were captured by the artificial astigmatic eye in each situation.

Ametropy compensation was first achieved by a programmed cylindrical lens displayed on the LCoS panel with the same orientation as the ophthalmic cylindrical lens used as $L_A$. According to Eq. (7), and keeping $d = 90$ mm, the calculated focal lengths to compensate for the horizontal and vertical ametropia were $f'_C = -594$ mm and $f'_C = +740$ mm, respectively. The focal length of the programmed lens displayed on the SLM was adjusted to experimentally optimize the compensation. The experimental focal lengths that best performed were $f'_C = -578$ mm and $f'_C = +813$ mm, respectively, which are in good agreement with the predicted values. Sharply focused images were obtained by the compensated artificial eye, and they can be seen in the left and central columns of Fig. 8(b).

Conventional compensation by ophthalmic trial lenses placed in front of the artificial eye while addressing a flat mirror to the SLM was also carried out. The available cylindrical trial lens of −1.5 D optical power was used to compensate for the simple myopic astigmatism because it was the closest to the calculated value of −1.52 D for a distance $d = 10$ mm. For the compensation of the simple hypermetropic astigmatism, a cylindrical lens of +1.5 D from the trial set was used, because, again, it was the available lens closest to the predicted value +1.48 D. Figure 8(c) contains the captured images after the compensation for the simple myopic astigmatism in the horizontal direction (left) and the simple hypermetropic astigmatism in the vertical direction (center) by these conventional ophthalmic trial lenses. The quality of these images is compared with the images obtained after the compensation done by the programmed lenses on the SLM, through the computation of the MTF curves [left and central plots of Fig. 8(d)]. In both cases, the best performance corresponds to the programmable compensating lenses displayed on the LCoS-SLM, whose MTF curves have a slower decrease in the frequency domain than the conventional trial lenses and are closer to the emmetropic behavior. In fact, the compensation of simple hypermetropic astigmatism (vertical) with a trial lens presents an MTF curve that reveals a pseudoresolution effect (side lobe centered at ≈0.65 cycles/pixel) with reversal contrast, thus indicating the mediocre quality of this compensation.

Numerical results are summarized in Table 1 for the cases of myopia, hypermetropia, simple myopic (horizontal), and simple hypermetropic (vertical) astigmatisms, for the sake of an easier comparison.

**Table 1** Refractive errors induced to the artificial eye and their compensations calculated for a compensating lens placed closely in front of the eye ($d = 10$ mm), which represents the position of the conventional trial lens (third column) and at a distance of $d = 90$ mm with the additional displacement produced by the parallel-plate equivalent to the BS, which represents the position of the programmable lens displayed on the LCoS-SLM. Values are provided in diopters (D). Their equivalent focal lenses in (mm) are also given in brackets.

| | | Compensation by ophthalmic lens | | Compensation by programmable lens (SLM) | |
|---|---|---|---|---|---|
| Ametropy | Ocular refraction | Theoretical | Available trial lens | Theoretical | Experimental |
| Spherical | | | | | |
| Myopia | +3 D (+333.3 mm) | −3.09 D (−323 mm) | −3 D (−333.3 mm) | −3.85 D (−260 mm) | −3.62 D (−276 mm) |
| Hyper-metropia | −3 D (−333.3 mm) | +2.91 D (+343 mm) | +3 D (+333.3 mm) | +2.46 D (+406 mm) | +2.50 D (+400 mm) |
| Simple astigmatism | | | | | |
| Horizontal myopic | +1.5 D (+666.6 mm) | −1.52 D (−657 mm) | −1.5 D (−666.6 mm) | −1.68 D (−594 mm) | −1.73 D (−578 mm) |
| Vertical hyper-metropic | −1.5 D (−666.6 mm) | +1.48 D (+677 mm) | +1.5 D (+666.6 mm) | +1.35 D (+740 mm) | +1.23 D (+813 mm) |

Astigmatism was also induced in an oblique meridian. A +1.5 D cylindrical lens was placed in front of the emmetropic eye at an angle of 20 deg approximately from the horizontal axis on clockwise direction, causing the blurred image displayed on Fig. 8(a, right). This experiment was conducted in order to evaluate the capability of a pixelated LCoS screen to compensate for this ametropy at any given orientation. A cylindrical lens of −1.5 D, or equivalently, of −594 mm focal length, was programmed in the SLM to compensate for the induced astigmatism. The cylindrical lens was adjusted by computer in both focal length and orientation angle, finding the best compensation for a focal length of −578 mm at an orientation of 20 deg clockwise from the horizontal direction. The obtained image is shown in Fig. 8(b, right) with sharp contours and well-defined details. Ophthalmic compensation was achieved by the use of a conventional cylindrical trial lens of −1.5 D, placed in front of the artificial eye, while addressing a constant value to the SLM that acted as a flat mirror. Image depicted in Fig. 8 (c, right) permits to visualize the achieved compensation. Comparison of the quality of the images is easily carried out by comparing the MTF values obtained from the captured focused images [Fig. 8(d, right)]. Again in this figure, the MTF curve corresponding to the programmable lens has a similar performance to the emmetropic eye and shows a less steep decrease than that corresponding to the conventional trial lens, just showing its better compensation quality.

Defocus has been compensated in the astigmatic artificial eye, but not distortion. Although it is hardly noticeable in the blurred images [Fig. 8(a)], distortion already affects the uncorrected images[20] and it depends on the location of the astigmatic lens that is being used to induce the astigmatism. The different locations of the compensating lenses $L_C$ and $L_C^*$ lead to different powers and also to different spectacle magnifications[20] that, in the end, produce different degrees of distortion in the compensated image. For example, in the case of astigmatism induced in an oblique meridian astigmatism [Fig. 8(b, right)], due to the longer distance ($d = 90$ mm) between the programmable compensating lens $L_C$ and the astigmatic artificial eye, the residual distortion effect is more noticeable in the image focused with the programmable lens than with the trial lens $L_C^*$. The latter was only at $d = 10$ mm from the lens that induced the oblique astigmatism. For the three cases of astigmatism considered in Fig. 8, we have computed the ratio ($D_{\text{Oph}}^{\text{SLM}}$) of the distortion produced by the programmable lens displayed on the modulator with respect to the ophthalmic trial lens, from the series of identities

$$D_{\text{Oph}}^{\text{SLM}} = \frac{\text{distortion}^{\text{SLM}}}{\text{distortion}^{\text{Oph}}} = \frac{\text{SM}_\alpha^{\text{SLM}}}{\text{SM}_\alpha^{\text{Oph}}} = \frac{\text{corrected image size}_\alpha^{\text{SLM}}}{\text{corrected image size}_\alpha^{\text{Oph}}}, \tag{8}$$

where $\alpha$ represents the meridian in which the astigmatism was induced (the perpendicular meridian remained unaffected in our experiments) and SM is the spectacle magnification (defined as the ratio of retinal image size in the corrected eye to the basic height of the retinal image in the uncorrected eye[20]). To obtain the last identity of Eq. (8), we have taken into account that, in all the cases considered, the retinal image in the uncorrected eye was the same for both types of compensations. From Eq. (8) and the experimental results of astigmatism compensation, we have obtained the following distortion ratios: $D_{\text{Oph}}^{\text{SLM}}(\text{horizontal}) = 0.892$ (12%) (Fig. 8, left); $D_{\text{Oph}}^{\text{SLM}}(\text{vertical}) = 1.135$ (13.5%) (Fig. 8, central); $D_{\text{Oph}}^{\text{SLM}}(\text{oblique}) = 0.889$ (12.5%) (Fig. 8, right).

Finally, presbyopia was the fourth experiment simulated in the optical bench. To do this, a near object was obtained by

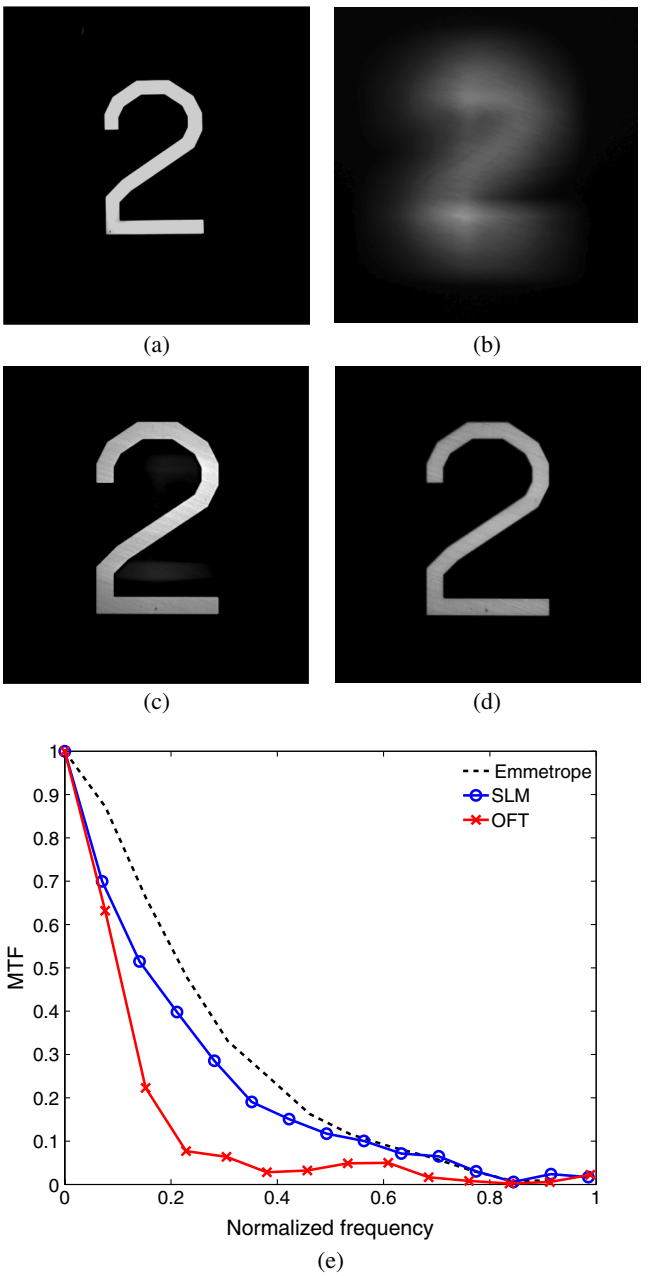


**Fig. 9** Experimental results of the compensation for presbyopia. (a) Reference: captured image of a distant object by the artificial emmetropic eye. (b) Defocused image of a near object (placed at 500 mm from the eye approximately) obtained when the presbyopic artificial eye has just +1 D of accommodation. (c) Refocused image after compensation with the programmable lens displayed on the SLM, which provided the necessary additional power (focal length finely tuned to +700 mm). (d) Refocused image after compensation by an ophthalmic trial lens with additional optical power of +1.5 D. (e) MTF curves corresponding to figures (a), (c), and (d).

approaching lens $L_1$ to the USAF test (O in Fig. 5) so that its conjugated image, which corresponds to test $A$ in Fig. 4, was located approximately at 500 mm from the artificial eye. In such a situation, the acquired image by the emmetropic eye was defocused, unless sufficient accommodation (about +2 D) was available. We assumed the accommodation capability was limited to just +1 D, that is, the artificial eye suffered from presbyopia. To simulate this presbyopia, a lens $L_P$ of +1 D was placed at the location of $L_X$ (Fig. 5) and a defocused image was captured as shown in Fig. 9(b). From the optical power of $L_P$ (or equivalently, its focal length $f'_P = 1000$ mm) and taking into account that the distance between the compensating lens and the artificial presbyopic eye was $d = 110$ mm, the necessary additional power of the compensating lens $L_C$ was +1.44 D, or equivalently, a +694 mm focal length [Eq. (5)]. Compensation for presbyopia was first attempted with the programmable lens displayed on the SLM. A range of focal lengths from +600 to +720 mm in steps of 5 mm were sequentially addressed to the LCoS device, obtaining the best compensation for $f'_C = +700$ mm, which corresponds to an optical power of +1.43 D. This result was nearly coincident with the theoretically predicted by calculation (+694 mm). The captured image after this compensation is shown in Fig. 9(c). After that, we applied the alternative compensation with a conventional trial lens. If a plane mirror was displayed on the SLM, and an ophthalmic trial lens of +1.5 D was used, the compensation was also achieved as shown in Fig. 9(d). Comparing both results in terms of MTF values [graphs depicted in Fig. 9(e)], a better performance of the programmable lens is obtained in comparison to the ophthalmic trial lens.

## 4 Discussion and Conclusions

A programmable lens displayed on an SLM can be used for ophthalmic compensation. More specifically, it can be advantageously used instead of conventional trial lenses in phoropters and trial spectacle frames because it has no need of moving components or replacing lenses and offers the possibility of finer tuning controlled by computer. Although the standard refractive uncertainty is 0.25 D and, most frequently, subjects cannot discriminate refractive errors below this figure,[15] we tuned more finely the optical power (focal length) of the programmable diffractive lens displayed on the SLM because this allowed us to obtain MTFs closer (and sometimes, slightly better) than those obtained with trial-set ophthalmic lenses. This is a nearly costless operation since the refreshment of the programmable compensating lens by the modulator is fast and does not require the physical replacement and alignment of any optical component. Likewise, ophthalmic thin prisms could be also displayed.

The proof of concept has experimentally shown these advantages for an artificial eye to which several kinds of refractive errors (myopia, hypermetropia, and astigmatism) and presbyopia had been induced. In the case of astigmatism, the orientation of the principal meridians was also detected by computer with no need of in-plane rotations of trial lenses.

This experimental demonstration in optical test bench paves the way to other applications where a customized ophthalmic compensation would be advantageous: for example, in a large variety of eyepieces joined to microscopes, binoculars, cameras, and other instruments (no generally portable).

The system used in this work is a proof of concept and, as such, it has been useful to validate the hypothesis although its many limitations. Some constraints, such as the need for polarized light, not high efficiency (zero-order diffraction efficiency about 60%), spectral response, reflective configuration, small aperture, alignment requirements, associated electronic control system that consumes energy from a power supply or battery, and various parameters concerning pixel pitch, and resolution have been already mentioned in Sec. 1 for general LCoS-SLM-based systems. Although reflective LCoS modulators performs better than the transmission modulators in essential features (phase-only modulation with $2\pi$-phase modulation range or higher, smaller pixel pitch and higher resolution), which allow the display of better quality programmable lenses in a wider range of optical powers, their reflective configuration becomes an important drawback for the system. Let us comment two disadvantages derived from the fact that the programmable lens has to be placed at a longer distance from the eye than in the transmission configuration: first, the pupil effects, which considerably reduce the field of view; and second, the increased distortion of the image at the sensor plane when compensating for astigmatism. Another important issue concerns the presence of severe chromatic aberrations when using diffractive lenses, since most of the applications of optical instruments require the use of white light. Some reported solutions to this problem rely on exploiting the multiplexing capacity and fast refreshing capability of SLMs.[5,22,23] Some other problems concerning customized compensation of high-order aberrations and extended depth of focus have also been addressed in the related literature.[11–13,24] A combined and effective solution would be closer if transmission modulators with improved specifications, similar to those of current reflective modulators, were available in the next future.

### Acknowledgments

This research has been partly funded by the Spanish Ministerio de Ciencia e Innovación and FEDER (Project DPI2009-08879).

### References

1. V. Laude, "Twisted-nematic liquid-crystal pixelated active lens," *Opt. Commun.* **153**(1–3), 134–152 (1998).
2. J. A. Davis et al., "Fresnel lens-encoded binary phase-only filters for optical pattern recognition," *Opt. Lett.* **14**(13), 659–661 (1989).
3. N. Fukuchi et al., "Lensless Vanderlugt optical correlator using two phase-only spatial light modulators," *Chin. Opt. Lett.* **7**(12), 1–3 (2009).
4. X. Zeng et al., "Compact optical correlator based on one phase-only spatial light modulator," *Opt. Lett.* **36**(8), 1383–1385 (2011).
5. M. S. Millán, J. Otón, and E. Pérez-Cabré, "Dynamic compensation of chromatic aberration in a programmable diffractive lens," *Opt. Express* **14**(20), 9103–9112 (2006).
6. D. A. Atchison, "Spectacle lens design: a review," *Appl. Opt.* **31**(19), 3579–3585 (1992).
7. C. W. Fowler and E. S. Pateras, "Liquid crystal lens review," *Ophthalmic Physiol. Opt.* **10**(2), 186–194 (1990).
8. L. N. Thibos and A. Bradley, "Use of liquid-crystal adaptive-optics to alter the refractive state of the eye," *Optom. Vision Sci.* **74**(7), 581–587 (1997).
9. G. Li et al., "Switchable electro-optic diffractive lens with high efficiency for ophthalmic applications," *Proc. Natl. Acad. Sci. U. S. A.* **103**(16), 6100–6104 (2006).
10. Coastal Vision website: http://www.coastalvisionva.com (19 December 2013).

11. S. Manzanera et al., "Liquid crystal adaptive optics visual simulator: application to testing and design of ophthalmic optical elements," *Opt. Express* **15**(24), 16177–16188 (2007).
12. E. J. Fernández, P. M. Prieto, and P. Artal, "Wave-aberration control with a liquid crystal on silicon (LCOS) spatial phase modulator," *Opt. Express* **17**(13), 11013–11025 (2009).
13. C. Schwarz et al., "Binocular adaptive optics vision analyzer with full control over the complex pupil functions," *Opt. Lett.* **36**(24), 4779–4781 (2011).
14. Holoeye website: http://holoeye.com/ (1 October 2013).
15. G. Smith, "Refraction and visual acuity measurements: what are their measurement uncertainties?," *Clin. Exp. Optometry* **89**(2), 66–72 (2006).
16. J. Otón, M. S. Millán, and E. Pérez-Cabré, "Programmable lens design in a pixelated screen of twisted-nematic liquid crystal display," *Opt. Pura Apl.* **38**(2), 47–56 (2005).
17. J. Otón et al., "Imaging characteristics of programmable lenses generated by SLM," in *CP860, Information Optics: 5th Int. Workshop*, G. Cristóbal, B. Javidi, and S. Vallmitjana, Eds., pp. 471–480, American Institute of Physics, Toledo, Spain (2006).
18. International Organization for Standardization (ISO), ISO 11979-2 Ophthalmic Implants, Intraocular Lenses. Part 2: Optical Properties and Test Methods, Geneva, Switzerland (1999).
19. S. Norrby et al., "Model eyes for evaluation of intraocular lenses," *Appl. Opt.* **46**(26), 6595–6605 (2007).
20. R. B. Rabbets, *Bennett & Rabbets' Clinical Visual Optics*, 4th ed., Butterworth-Heinemann Elsevier, Edinburgh (2007).
21. J. Otón et al., "Multipoint phase calibration for improved compensation of inherent wavefront distortion in parallel aligned liquid crystal on silicon displays," *Appl. Opt.* **46**(23), 5667–5679 (2007).
22. A. Márquez et al., "Achromatic diffractive lens written onto a liquid crystal display," *Opt. Lett.* **31**(3), 392–394 (2006).
23. M. S. Millán, J. Otón, and E. Pérez-Cabré, "Chromatic compensation of programmable Fresnel lenses," *Opt. Express* **14**(13), 6226–6242 (2006).
24. L. A. Romero et al., "Double peacock eye optical element for extended focal depth imaging with ophthalmic applications," *J. Biomed. Opt.* **17**(4), 046013 (2012).



**María S. Millán** received her PhD degree in physics in 1990. She is a full professor in the College of Optics and Optometry at the Technical University of Catalonia (Barcelona, Spain). Her research work on image processing involves optical and digital technologies, algorithms, and development of new applications to industry and medicine. She has been a representative of the Spanish Territorial Committee in the International Commission for Optics. She is a member of OSA and Fellow member of SPIE and EOS.

**Elisabet Pérez-Cabré** is currently an associate professor at the Universitat Politècnica de Catalunya (UPC), Spain. She received her BSc and the PhD degrees in physics in 1993 and 1998, respectively. Her main research interests include color pattern recognition, optical encryption, and diffractive optics. She was promoted to SPIE Senior Member in 2011 for achievements in optical information processing and security systems.

**Lenny A. Romero** is currently an assistant professor at the Universidad Tecnológica de Bolívar, Colombia. She received her BSc degree in physics at the Universidad Industrial de Santander, Colombia, in 2004, and her PhD degree in optical engineering at the Universitat Politècnica de Catalunya, Spain, in 2013.

**Natalia Ramírez** received her BSc degree in physical engineering at the Universidad EAFIT, Colombia in 2013.